Acta Chemica Scandinavica, 1997: 51: 904–909
Printed in UK – all rights reserved

ACTA
CHEMICA SCANDINAVICA
ISSN 0904–213X

Effect of Non-Stoichiometry on Properties of $La_{1-t}MnO_{3+\delta}$. Part II. Crystal Structure

Natsuko Sakai,[a,†] Helmer Fjellvåg[a,*] and Bente Lebech[b]

[a]Department of Chemistry, University of Oslo, N-0315 Oslo, Norway and [b]Department of Solid State Physics, Risø National Laboratory, DK-4000 Roskilde, Denmark

Sakai, N., Fjellvåg, H. and Lebech, B., 1997. Effect of Non-Stoichiometry on Properties of $La_{1-t}MnO_{3+\delta}$. Part II. Crystal Structure. – Acta Chem. Scand. 51: 904–909. © Acta Chemica Scandinavica 1997.

Crystal structure data at 298 K were deduced from high-resolution powder neutron diffraction measurements of seven samples within the homogeneity range of the grossly non-stoichiometric $La_{1-t}MnO_{3+\delta}$ phase. During simultaneous refinements of powder X-ray (synchrotron) and neutron diffraction data for $La_{0.96}MnO_{3.05}$ several simple and complex defect models were tested out. There is no significant evidence for a more complex model than random vacancies at the La and Mn sites. The refined composition $La_{0.979}MnO_{3.057}$ proves the existence of unequal amounts of vacancies at the La and Mn sites. The fully reduced $La_{1-t}MnO_{3-3t/2}$ samples contain solely Mn^{III}. The degree of Jahn–Teller distortion for the reduced samples having an orthorhombic structure (ORT1-type; space group *Pnma*) is independent of the concentration of La and O vacancies. The more oxidized samples with 10–30% Mn^{IV} take either the $GdFeO_3$ (*Pnma*) or the $LaAlO_3$-type (*R-3c*) structure, both with regular MnO_6 octahedra. The valency of Mn is discussed on the basis of bond strength considerations.

Lanthanum manganese oxide, $LaMnO_{3+\delta}$, exhibits oxidative non-stoichiometry.[1] Few such perovskites are known. Some of these, like $La_5Ti_5O_{17}$, exhibit superstructures,[2] whereas the non-stoichiometry in others, like $LaMnO_{3+\delta}$, involves randomly distributed cation vacancies.[3–5] Interest in materials related to $La_{1-t}MnO_{3+\delta}$ stems from their potential use, e.g. in solid oxide fuel cells. In this context, the effect of temperature and oxygen partial pressure on details of the crystal structure is of relevance. The existence conditions for three modifications of $La_{1-t}MnO_{3+\delta}$ were described in Part I of this study and in recent publications.[1,6–8] Two of these take orthorhombic structures (ORT1 and ORT2, with space group *Pnma*; with and without Jahn–Teller deformed MnO_6 octahedra). The third type is rhombohedral (RH-type; $LaAlO_3$-type structure).[6,9] Their appearance during synthesis depends on the temperature, on oxygen partial pressure conditions during annealing and on cooling procedures. Temperature-induced phase transitions between these modifications are of first order. The ORT1 → ORT2 → RH transitions involve modest shifts of atomic positions, no reconstructions are required and the transitions are believed to be rapid. This implies that the structural situation conveyed by quenched samples can differ from that prevailing under *in situ* conditions.[6]

The commonly accepted defect model for oxygen-exessive $La_{1-t}MnO_{3+\delta}$ assumes vacancies on the metal sublattices. This view is based on the variation of the non-stoichiometry as a function of temperature and oxygen partial pressure,[1,10] supported by density and powder neutron diffraction data.[3,4,11] Tofield and Scott[3] found from powder neutron diffraction data vacancies on the La and the Mn sublattices in a ratio of 3:1 for $LaMnO_{3.12}$. Later, van Roosmalen *et al.*[4] reported equal amounts of vacancies on these two sublattices for $LaMnO_{3.158}$, and questioned, based on the compositional dependence of unit cell dimensions, the initial La/Mn ratio of the sample studied by Tofield and Scott. The defect model by Kuo *et al.*[5] is in agreement with the newer findings by van Roosmalen *et al.*; however, the models by Shimoyama *et al.*[12] and Mizusaki *et al.*[7] are substantially different.

$LaMnO_{3+\delta}$ has been studied by high-resolution electron microscopy. A lack of diffuse scattering and no indications of extended defects indicate that no defect clustering occurs for $\delta \geq 0$.[4,13] On the other hand, for oxygen-deficient $La_{1-t}MnO_{3+\delta}$ with $\delta < 0$, HREM show interactions between point defects for defect concentrations above 0.1%.[13,14]

The powder neutron diffraction studies by Tofield and Scott[3] and van Roosmalen *et al.*[4] concerned solely the

† Present address: Department of Inorganic Materials, National Institute of Materials and Chemical Research, 1-1 Higashi, Tsukuba, Ibaraki 305, Japan.
* To whom correspondence should be addressed.

rhombohedral modification. The Jahn–Teller distorted orthorhombic ORT1 variant has attracted substantial attention at an earlier stage,[15,16] whereas data are lacking for the ORT2 structure and for La-deficient $La_{1-t}MnO_{3+\delta}$.

The structural properties of non-stoichiometric $La_{1-t}MnO_{3+\delta}$ are presently addressed on the basis of high-resolution powder neutron and X-ray diffraction data. The motivation for the study is manyfold; to complete the description of modifications of $La_{1-t}MnO_{3+\delta}$, to provide crystal structure data for La-deficient materials, possibly to identify correlations between defects and structure type and, in particular, to verify the defect structure of $La_{0.96}MnO_{3.05}$ by means of combined refinements of high-resolution powder X-ray and neutron diffraction data (extending to high $\sin\Theta/\lambda$). Presently, results from neutron diffraction are reported for representative samples of the entire non-stoichiometric domain. Earlier results have frequently been extracted from data covering a limited $\sin\Theta/\lambda$ range, which imply that derived occupation numbers are somewhat uncertain. Finally, reported weak, non-explained, superstructure reflections[4] address questions concerning unit cell and space group.

Experimental

Powder samples (10–20 g) of $La_{1.00}MnO_{3.00}$, $La_{1.00}MnO_{3.08}$, $La_{1.00}MnO_{3.15}$, $La_{0.96}MnO_{2.94}$, $La_{0.96}MnO_{3.05}$, $La_{0.92}MnO_{2.88}$ and $La_{0.92}MnO_{2.98}$ were prepared from titrated aqueous solutions of $LaCl_3$ and $MnCl_2$ as described in Ref. 6. The oxygen contents of the individual single-phase oxides were monitored in a final heat treatment. Oxygen potentials during annealing were monitored by an oxygen sensor of Y_2O_3-stabilized ZrO_2.

The oxygen contents of all samples were determined from reoxidation experiments using thermogravimetry (TG; Perkin Elmer TGA7 system). E.g., for $La_{0.96}MnO_{3.05}$ synthesized by annealing in oxygen at 1273 K, the oxygen content was analyzed by first annealing the sample in H_2/CO_2 atmosphere at $p(O_2) = 10^{-7}$ Pa. Thereafter the sample was cooled to 293 K while maintaining the atmosphere. The obtained product $La_{0.96}MnO_{2.94}$ was thereafter reoxidized on heating in O_2 to 1273 K. Any possible, but not probable, kinetic decomposition of $LaMnO_3$ or formation of Mn^{II} is ignored. The determined oxygen content is 3.05 ± 0.01. The La/Mn ratio is based on titration of mother solutions used in the synthesis. For $MnCl_2$, EDTA was used as chelating agent and Eriochrome Black T as an indicator at pH 10. For $LaCl_3$, back titrations were done using EDTA and $ZnSO_4$ standard solutions. The precision in the titrations is within 0.3%. Considering also possible errors in pipets and in loss of manganese owing to non-complete precipitation, the precision in the La/Mn-mass determination is within 0.5%.

Samples annealed in O_2 at 1000 K with subsequent oxygen saturation during slow cooling take a rhombohedral structure. Samples quenched in air from, say, 1273 K are of the orthorhombic ORT2-type, whereas orthorhombic ORT1-type samples are obtained after annealing (and cooling) in reducing atmosphere, $p(O_2) = 10^{-7}$ Pa ($Ar/CO_2/H_2$ at 1270 K). For further details see Ref. 6. The reduced samples did not reoxidize significantly during handling, storage and experiment in air at room temperature.

All samples were characterized with respect to phase purity, sample homogeneity and unit-cell dimensions with powder X-ray diffraction (Guinier–Hägg cameras, Cu $K\alpha_1$ radiation, Si as internal standard, $a = 543.01$ pm[17]).

Powder neutron diffraction data at 298 K were collected at Risø National Laboratory, Roskilde, Denmark, using the TAS III instrument in the multidetector powder diffraction mode. Monochromatized neutrons with wavelengths $\lambda = 145.05$ and 224.2 pm were obtained by reflection from Ge(311) and Ge(511). Scattered neutrons were registered by a bank of 20 ^{3}He detectors, positioned 5.2897° apart. The range 5–115.79° was covered by moving the detector bank 5.2897° during 100 steps. The individual detectors were calibrated by intensity data recorded for a heavily scattering polymer. Cylindrical sample holders of vanadium were used. Atomic coordinates, isotropic displacement factors and occupation numbers were obtained from Rietveld-type refinements. Owing to strong correlation between displacement and occupation parameters, as many as possible of these were fixed or constrained at reasonable values during (preliminary) stages of the refinements. Since the refined occupation numbers were close to those expected from the nominal composition, the occupation numbers were fixed during the final refinements. A Gaussian peak shape function was used, although the instrumental peak shape deviates from this function, especially for scattering angles below 30°. The ALLHKL and EDINP,[18] and the Hewat[19] versions (intensity data approximated to integer steps in 2Θ) of the Rietveld program were used. The scattering amplitudes $b_{La} = 8.27$, $b_{Mn} = -3.73$ and $b_O = 5.805$ fm were adopted.[20]

Powder X-ray diffraction data were collected for $La_{0.96}MnO_{3.05}$ at the Swiss–Norwegian beam line (SNBL), BM1, at the European Synchrotron Radiation Facility, Grenoble. X-Rays of wavelength 89.987 pm were obtained by reflection from a Si(111) channel cut monochromator. The GSAS program[21] was used for simultaneous refinements of the powder X-ray data from ESRF and the neutron data from Risø (wavelength 145.05 pm). The observed X-ray and neutron peak profiles were described by pseudo-Voigt functions, and the backgrounds were modelled by cosine Fourier-series polynomials. The unit-cell dimensions, atomic coordinates and (fixed) occupation numbers determined for $La_{0.96}MnO_{3.05}$ by means of the Risø data were used as starting point for the refinements. The displacement

factor for Mn (and for O) in different possible sites were constrained to the same value.

Results and discussion

(i) *Average structure for* $La_{1-t}MnO_{3+\delta}$. Magnetic susceptibility data showed that the magnetic ordering temperatures for the studied samples are below 260 K. Hence, there are no magnetic contributions to the observed neutron diffraction profiles. During the final part of the profile refinements, the occupation numbers were constrained to fit the nominal composition. This was found adequate, since interstitials and misplaced atoms are not important for the defect situation, see section (ii). The derived atomic coordinates for the average structure were found not to depend strongly on details in the defect description. The results are presented for the orthorhombic (ORT1, ORT2) and rhombohedral (RH) modifications in Tables 1–3. For samples with $\delta \geqslant 0.00$, a completely filled oxygen sublattice is used as the reference level ($n_O = 1.00$), whereas for samples with $\delta < 0.00$ a completely filled Mn sublattice acts as reference level ($n_{Mn} = 1.00$).

The reduced samples with solely Mn^{III} take the Jahn–Teller distorted orthorhombic ORT1 structure. Any La deficiency in such samples implies that δ will be negative. This situation was modelled by assuming random La and O vacancies. The refinements gave no conclusive results for any preferred distribution of the vacancies over the O1 and O2 sites. The obtained parameters and interatomic distances are given in Tables 1 and 3. The projection of the crystal structure on the *ac*-plane in Fig. 1 (cf. also Table 3) shows that the MnO_6 octahedra are deformed into a 4+2 situation with alternating orientation of the square planar (central) part of the octahedra.

Samples quenched from intermediate to high temperatures contain 10–15% Mn^{IV} and take the orthorhombic ORT2 structure. The results for $LaMnO_{3.08}$ are included in Tables 1 and 2. The type of tilting of the octahedra are the same for the orthorhombic ORT1 and ORT2

Table 2. Unit-cell dimensions from powder X-ray diffraction and atomic coordinates, displacement factors and occupation numbers for the rhombohedral variant of $La_{1-t}MnO_{3+\delta}$ as derived from Rietveld refinements of powder neutron diffraction data collected at the Risø reactor, Denmark.[a]

	$La_{0.96}MnO_{3.05}$	$La_{0.92}MnO_{2.98}$
a/pm	547.4(1)	547.7(1)
α/°	60.640(5)	60.614(5)
x_O	0.8005(4)	0.8026(5)
B(La)	0.68(6)	0.23(6)
B(Mn)	0.37(11)	0.48(1)
B(O)	0.96(5)	0.86(6)
n(La)	0.9449[b]	0.92[b]
n(Mn)	0.9843[b]	1.00[b]
n(O)	1.0[b]	0.993[b]
R_n	6.14	9.16
R_p	12.69	16.92

[a]Calculated standard deviations are given in parentheses. Nuclear (F^2) and profile *R*-factors[19] are given, R_n and R_p. Space group *R-3c*, La in 2(*a*) [1/4, 1/4, 1/4], Mn in 2(*b*) [0, 0, 0] and O in 6(*e*) [*x*, $-x+1/2$, 1/4]. [b]Fixed; are relative numbers, see text.

Table 1. Unit-cell dimensions from powder X-ray diffraction and atomic coordinates, displacement factors and occupation numbers for the orthorhombic ORT1- and ORT2-type variants of $La_{1-t}MnO_{3+\delta}$ at $T = 298$ K as derived from Rietveld refinements of powder neutron diffraction data collected at the Risø reactor, Denmark.[a]

	$La_{1.00}MnO_{3.00}$ ORT1	$La_{0.96}MnO_{2.94}$ ORT1	$La_{0.92}MnO_{2.88}$ ORT1	$La_{1.00}MnO_{3.08}$ ORT2
a/pm	573.6(1)	573.2(2)	573.0(1)	549.7(2)
b/pm	770.3(2)	769.0(2)	769.5(2)	779.4(2)
c/pm	554.0(1)	553.7(1)	553.4(1)	553.2(2)
x_{La}	0.0494(8)	0.0495(8)	0.0480(7)	0.0228(8)
z_{La}	0.9913(8)	0.9935(9)	0.9906(8)	0.9975(14)
x_{O1}	0.4876(10)	0.4854(9)	0.4886(8)	0.4937(13)
z_{O1}	0.0729(10)	0.0768(9)	0.0752(9)	0.0661(13)
x_{O2}	0.1956(7)	0.1940(7)	0.1955(6)	0.2252(10)
y_{O2}	0.5397(5)	0.5400(5)	0.5402(5)	0.5354(6)
z_{O2}	0.2280(7)	0.2231(7)	0.2243(6)	0.2252(10)
B(La)	0.27(6)	0.71(8)	0.40(12)	0.66(6)
B(Mn)	0.54(19)	0.18(12)	0.60(19)	0.30(8)
B(O1,O2)	0.34(13)	0.34(5)	0.54(16)	0.98(10)
n(La)	1.00[b]	0.96[b]	0.92[b]	0.9737[b]
n(Mn)	1.00[b]	1.00[b]	1.00[b]	0.9737[b]
n(O1)	1.00[b]	0.98[b]	0.96[b]	1.00[b]
n(O2)	1.00[b]	0.98[b]	0.96[b]	1.00[b]
R_n	7.8	9.83	8.1	8.5
R_p	19.7	19.1	17.5	19.1

[a]Calculated standard deviations are given in parentheses. Nuclear (F^2) and profile *R*-factors[19] are given, R_n and R_p. Space group *Pnma*; La and O(1) in 4(*c*) [*x*, 1/4, *z*], Mn in 4(*a*) [0, 0, 1/2] and O(2) in 8(*d*) [*x*, *y*, *z*]. [b]Fixed; are relative numbers, see text.

Table 3. Calculated distances (in pm) for selected samples of $La_{1-t}MnO_{3+\delta}$ based on unit-cell dimensions and atomic coordinates determined from powder neutron diffraction data at 298 K.[a]

Composition structure type	$LaMnO_{3.15}$ RH	$La_{0.96}MnO_{3.05}$ RH	$LaMnO_{3.08}$ ORT2	$LaMnO_{3.00}$ ORT1
La–O2 (2×) La–O1 (1×)	247.6 (×3)	248.4 (×3)	248.5 241.9	246.5 244.0
La–O2 (2×) La–O1 (1×)	274.5 (×3)	275.1 (×3)	264.2 261.6	262.5 255.4
La–O2 (2×) La–O1 (1×)	275.6 (×3)	275.1 (×3)	278.8 293.3	272.1 314.6
La–O1 (1×) La–O2 (2×)	304.6 (×3)	304.3 (×3)	312.1 315.8	325.4 339.4
Mn–O2 (2×) La–O1 (2×) La–O2 (2×)	195.7 (×6)	196.5 (×6)	198.0 198.3 197.7	190.3 196.9 217.7
v(Mn) $v(Mn_{expected})$	3.360 3.30	3.286 3.22	3.154 3.16	2.994 3.00

[a]O1 and O2 are equivalent for the rhombohedral (RH) phase. Calculated bond strengths (valence) are given for Mn (see text). Calculated standard deviations are typically 0.7 pm for La–O, and 0.2 pm for Mn–O bonds.

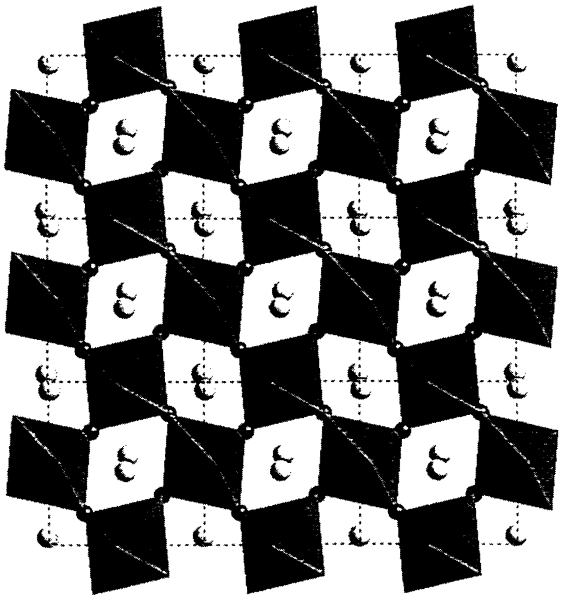

Fig. 1. Projection of the orthorhombic (ORT1) crystal structure of $LaMnO_{3.00}$ on the *ac*-plane (*X* is vertical).

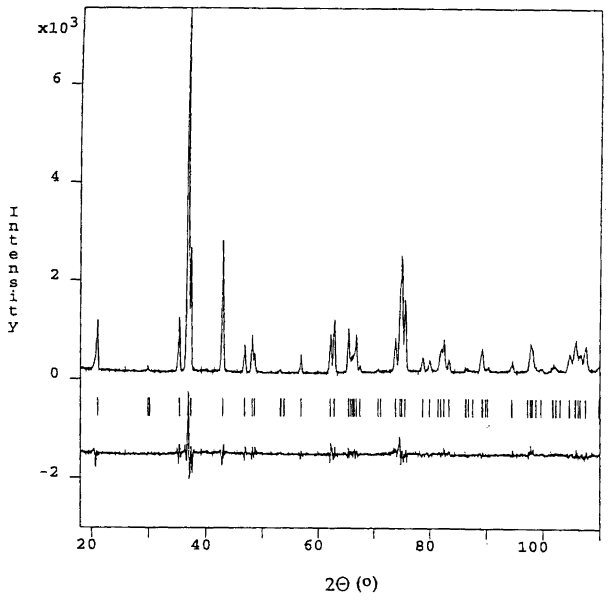

Fig. 2. Observed and difference powder neutron diffraction pattern for rhombohedral $La_{0.96}MnO_{3.05}$ at 298 K, $\lambda = 145.05$ pm. Position of Bragg reflections marked by vertical bars.

structures.[22] However, for the ORT2-type, the MnO_6 octahedra are regular (Table 3).

The oxygen saturated samples take the rhombohedral structure. Results are given in Tables 2 and 3. The values for x_O fit well earlier findings.[3,4,23] The additional reflections reported[4] in the neutron diffraction powder pattern for $LaMnO_{3.158}$ at $d = 214$, 209 and 185 pm were presently not observed. Although some of these coincide with additional peaks appearing when $LaMnO_{3.15}$ undergoes the rhombohedral to orthorhombic (ORT2) phase transition just below room temperature,[9,24] their origin must still be considered unknown. The observed and difference powder neutron diffraction patterns are shown for $La_{0.96}MnO_{3.05}$ in Fig. 2.

Larger changes in the valence state of manganese will be reflected in the Mn–O interatomic distances.[25] Such valence changes can be estimated by means of the bond strength concept.[26] The calculated changes can further be compared with variations deduced from thermogravimetric analyses of the (bulk) oxygen content. In the calculations, the tabulated value 1.76 for manganese[26] was adjusted to 1.742 in order to provide perfect matching between expected and calculated valence for

$LaMnO_{3.00}$ (Table 3). The relative variation is rather independent of this choice, however, for certain perovskites, e.g. $LaCoO_3$, it is well known that tabulated parameters overestimate the valence of the *d*-element. The good agreement between calculated and expected valence (Table 3) provides independent support to the claim that major valence changes for the octahedral Mn atoms are important for the charge balance.

(ii) *Models for gross non-stoichiometry. Refinement of the defect structure of $La_{0.96}MnO_{3.05}$ from powder X-ray and neutron diffraction data.* Several simple defect models were considered by van Roosmalen *et al.*[4] during refinements of powder neutron diffraction data for $LaMnO_{3.158}$, *inter alia*: (1) La vacancies; (2) Mn vacancies; (3) vacancies in unequal amounts at the La and Mn sites (i.e. as described by Tofield and Scott[3]); and (4) vacancies in equal amounts at the La and Mn sites:

$$LaMnO_3 + \delta/2\ O_2 \rightarrow (3+\delta)/3[La_{3/(3+\delta)}V_{\delta/(3+\delta)})(Mn_{3/(3+\delta)}V_{\delta/(3+\delta)}O_3]$$

where V denotes a vacancy. Model (4) was favoured by the data. Also Kuo *et al.*[5] described the defect chemistry of $LaMnO_{3+\delta}$ according to model (4).

A charge disproportionation, $2\,Mn^{III} \rightarrow Mn^{II} + Mn^{IV}$, has been proposed at high temperatures. Unless charge ordering occurs, it will not influence the present defect description. It should be mentioned that charge ordering occurs for substituted $LaMnO_3$, e.g. for $La_{0.5}Ca_{0.5}Mn^{III}Mn^{IV}O_3$. Mizusaki *et al.*[7] described a different model for $La_{1-t}MnO_{3+\delta}$ where oxygen excess is associated with: (5) vacancies in equal amounts at the La and Mn sites plus redistribution of Mn atoms to La sites:

$$\{La_{3(2-x)/[(2-x)(3+\delta)]}Mn_{3x/[(2-x)(3+\delta)]}\}_A(Mn_{3/(3+\delta)})_BO_3$$

A and B denoting La and Mn sublattices, respectively. Shimoyama *et al.*[12] proposed: (6) La vacancies in combination with O vacancies, e.g. $La_{0.9}MnO_{2.85+\delta}$.

Models with interstitial Mn atoms have been considered improbable from electrostatic reasons,[4] since some Mn atoms then will have LaO_3 and La_2O_4 as close neighbours. This is only valid as long as single interstial atoms are considered. In more complex models, an interstitial Mn atom being part of a larger defect cluster appears energetically as more likely. It should be noted that there exists no experimental evidence from electron microscopy for defect clustering in oxygen excessive samples.[4,13]

Within the close packed LaO_3 part of the structure, Mn atoms occupy a subset of octahedral voids solely surrounded by O atoms. The (random) La site vacancies in the ccp sublattice of $La_{1-t}MnO_{3+\delta}$ may in principle be filled with oxygen atoms. However, interstitial Mn atoms are then required for providing chemical bonding for the additional oxygen. An additional O atom at a vacant La site provides locally tetrahedral, interstial Mn sites (Fig. 3) at (x, x, x), $x=0.1225$ and (x, y, z), $x \approx 0.125$, $y \approx 0.675$, $z \approx 0.575$. Filling of such Mn_{tetr} sites will require an empty neighbouring regular Mn site (face sharing polyhedra). Interstitial, octahedral Mn sites at (1/2, 0, 0) may exist, provided that two additional O atoms enter neighbouring vacant La sites (Fig. 3). The two last models considered are then: (7) interstitial Mn_{tetr} plus one O atom at vacant La site, and (8) interstitial Mn_{oct} plus O atoms at two neighbouring vacant La sites.

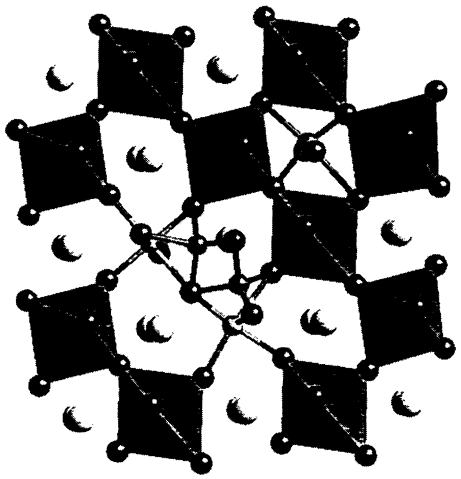

Fig. 3. Possible interstitial tetrahedral and octahedral Mn sites appearing locally when oxygen atoms enter one or two vacant (neighbouring) La sites. Projection on the *ac*-plane, see also Fig. 1.

Models (1)–(8) and all combinations of vacancies at La sites, misplaced oxygen atoms at La sites, Mn vacancies and Mn in new tetrahedral and octahedral sites, were tested out by simultaneous Rietveld type refinements (GSAS)[21] of powder X-ray and neutron diffraction data for $La_{0.96}MnO_{3.05}$. Whereas the scattering in the powder X-ray diffractogram is dominated by La and Mn, the situation is quite different in the neutron case with a strong scattering contribution from O and negative scattering amplitude for Mn. Therefore $La_{0.96}MnO_{3.05}$ with significant La deficiency and large oxygen surplus is well suited for a detailed analysis. However, a prerequisite for evaluation of the refinements is phase purity and correctness of the sample composition. Based on careful analyses (see Experimental), X-ray diffraction and magnetic susceptibility measurements, impurities of Mn_3O_4 were ruled out and the composition is evaluated as $La_{0.960\pm0.005}Mn_{1.000\pm0.005}O_{3.05\pm0.01}$.

No significant improvement in the reliability factors were obtained on turning from the simplest model with random La and Mn vacancies to the complex models (7) and (8). The data are not compatible with models (1), (2), (5) and (6). The combined powder X-ray and neutron diffraction study supports the defect model in Ref. 4; however, the vacancy concentrations are clearly different at the La and Mn sites. The refined occupation numbers suggest the overall chemical formula $La_{0.979(6)}MnO_{3.057(21)}$. Its La content is significantly larger than indicated by the nominal composition

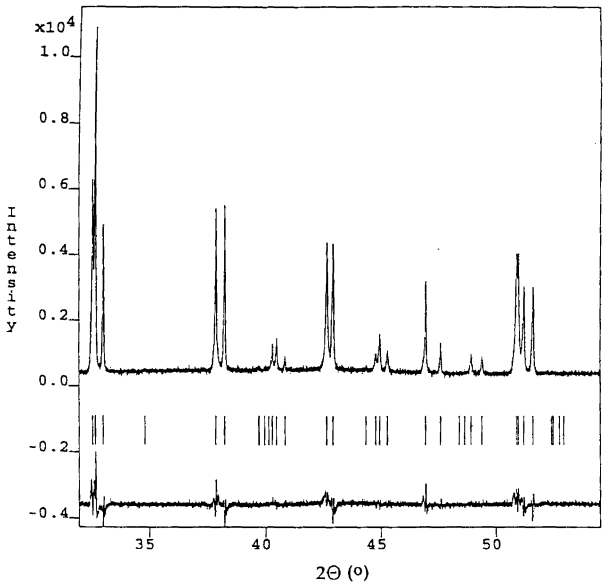

Fig. 4. Observed and difference powder X-ray diffraction pattern for rhombohedral $La_{0.96}MnO_{3.05}$ at 298 K, $\lambda =$ 89.987 pm, for the 2Θ range 30–55°. Position of Bragg reflections marked by vertical bars.

$La_{0.96}MnO_{3.05}$. This discrepancy is certainly not caused by Mn entering the La site [cf. model (5)], since in that case the opposite signs in neutron scattering amplitudes for La and Mn would have resultated in too low a refined La content. The chemical content of the rhombohedral unit cell is $La_{1.922}Mn_{1.962}O_{6.00}$.

The peak profiles in the X-ray pattern show significant broadening with substantial non-Gaussian contributions (Fig. 4). This probably reflects strain induced during sample preparation owing to a strong temperature dependence of the non-stoichiometry. In order to conclusively settle the question raised by the La site occupation numbers, similar sets of X-ray and neutron diffraction data are required for other stoichiometries and related structure types (ORT1 and ORT2); however, extreme care should be taken during synthesis to minimize peak broadening.

Acknowledgement. This work has received financial support form the Research Council of Norway. This is Contribution no. 97.01 from the Swiss–Norwegian Beam Line at ESRF, Grenoble.

References

1. van Roosmalen, J. A. M. and Cordfunke, E. H. P. *J. Solid* State Chem. *110* (1994) 109.
2. Williams, T., Schmalle, H., Reller, A., Lichtenberg, F., Widmer, D. and Bednorz, G. *J. Solid State Chem. 93* (1991) 534.
3. Tofield, B. C. and Scott, W. R. *J. Solid State Chem. 10* (1974) 183.
4. van Roosmalen, J. A. M., Cordfunke, E. H. P., Helmholdt, R. B. and Zandbergen, H. W. *J. Solid State Chem. 110* (1994) 100.
5. Kuo, J. H., Anderson, H. U. and Spalin, D. M. *J. Solid State Chem. 83* (1989) 62.
6. Sakai, N. and Fjellvåg, H. *Acta Chem. Scand. 50* (1996) 580.
7. Mizusaki, J., Tagawa, H., Yonemura, Y., Minamiue, H. and Nambu, H. In Ramaranayanan, T. A., Worrell, W. L. and Tuller, H. L., Eds., *Proceedings 2nd International Symposium on Ionic and Mixed Conducting Ceramics, The Electrochemical Soc. Proceeding 94–12*, 1994, p. 402.
8. Takeda, Y., Nakai, S., Kojima, T., Kanno, R., Imanishi, N., Shen, G. Q. Yamamoto, O., Mori, M. and Abe, T. *Mater. Res. Bull. 26* (1991) 153.
9. Hauback, B. C., Fjellvåg, H. and Sakai, N. *J. Solid State Chem. 121* (1996) 202.
10. Stevenson, J. W., Nasrallah, M. M., Anderson, H. U. and Sparlin, D. M. *J. Solid State Chem. 102* (1993) 185.
11. van Roosmalen, J. A. M. and Cordfunke, E. H. P. *J. Solid State Chem. 110* (1994) 106.
12. Shimoyama, J., Mizusaki, J. and Fueki, K. *Proc. Fall Meeting Chem. Soc. Jpn. 3Q06* (1986).
13. Mrowec, S. *Ceramurgia Int. 4* (1978) 47.
14. van Roosmalen, J. A. M. and Cordfunke, E. H. P. *J. Solid State Chem. 93* (1991) 212.
15. Koehler, W. C. and Wollan, E. O. *J. Phys. Chem. Sol. 2* (1957) 100.
16. Matsumoto, G. *J. Phys. Soc. Jpn. 29* (1970) 606.
17. JCPDS, Powder Diffraction File No 5–565.
18. Pawley, G. S. *Program ALLHKL*, Department of Physics, Edinborough University, Scotland 1981 [see also *J. Appl. Crystallogr. 14* (1981) 357].
19. Hewat, A. W., The Rietveld Computer Program for the Profile Refinement of Neutron Diffraction Powder Patterns Modified for Anisotropic Thermal Vibrations, *UKAERE HarwellReport* RRL 73/897, 1973.
20. L. Koester and H. Rauch, IAEA Contract 2517/RB, IAEA, Vienna 1981.
21. Larson, A. C. and Von Dreele, R. B., *Program GSAS – Generalized Structure Analysis System*, Los Alamos National Laboratory, Los Alamos, NM.
22. Glazer, A. M. *Acta Crystallogr., Sect. B 28* (1972) 3384.
23. Norby, P., Krogh Andersen, I. G., Krogh Andersen, E. and Andersen, N. H. *J. Solid State Chem. 119* (1995) 191.
24. Wold, A. and Arnott, R. J. *J. Phys. Chem. Sol. 9* (1959) 176.
25. Krogh Andersen, I. G., Krogh Andersen, E., Norby, P. and Skou, E. *J. Solid State Chem. 113* (1994) 320, and personal communication.
26. Brese, N. E. and ÒKeeffe, M. *Acta Crystallogr., Sect. B 47* (1991) 192.

Received November 20, 1996.